Soft Matter

Cite this: *Soft Matter*, 2012, **8**, 10167

www.rsc.org/softmatter

PAPER

Stimuli-responsive micellar interpolyelectrolyte complexes – control of micelle dynamics *via* core crosslinking†

Eva Betthausen,[a] Markus Drechsler,[a] Melanie Förtsch,[a] Dmitry V. Pergushov,[b] Felix H. Schacher*[c] and Axel H. E. Müller*[a]

Received 26th May 2012, Accepted 20th July 2012
DOI: 10.1039/c2sm26221e

Multi-layered micellar interpolyelectrolyte complexes (IPECs) were built up by the complexation of two oppositely charged homo- or block copolymer systems. First, an ampholytic polybutadiene-*block*-poly(sodium methacrylate)-*block*-poly{2-[(methacryloyloxy)-ethyl]trimethylammonium methylsulfate} (PB-*b*-PMANa-*b*-PDMAEMAq) ABC triblock terpolymer formed stimuli-responsive micelles in a pH 10 aqueous solution with a soft PB core, a PMANa/PDMAEMAq intramicellar IPEC (*im*-IPEC) shell, and a positively charged PDMAEMAq corona. With the addition of either negatively charged homopolymers (poly(sodium 4-styrenesulfonate) (PSSNa)) or bis-hydrophilic block copolymers comprising a neutral segment (poly(sodium acrylate)-*block*-poly(*N*-isopropylacrylamide) (PANa-*b*-PNIPAAm)), a second IPEC shell was formed. The structure of the resulting complex particles at different ratios of oppositely charged segments was investigated using cryogenic transmission electron microscopy (cryo-TEM) and dynamic light scattering (DLS). We show that the initial terpolymer micelles with the *im*-IPEC shell exhibit significant dynamic behavior upon further complexation, resulting in changes in core size distribution and aggregation number. We attribute this to the soft core-forming PB block. Upon crosslinking of the PB core such dynamic processes are suppressed, thus more uniform IPEC particles are formed. We further demonstrate that the PNIPAAm corona formed after complexation with PANa-*b*-PNIPAAm diblock copolymers renders these multicompartment particles thermo-responsive.

Introduction

The successful build-up of multifunctional macromolecular architectures using co-assembly processes has been one of the major objectives in polymer science within the last two decades. Thereby, one elegant and straightforward approach to direct these processes and, at the same time, provide utmost control over the properties of the resulting architectures, is to exploit electrostatic interactions. More specifically, the mixing of two oppositely charged polyelectrolytes leads to the spontaneous formation of interpolyelectrolyte complexes (IPECs).[1–6] The main driving force for complex formation in aqueous media is the entropy gain caused by the release of the low molecular weight counterions. IPEC formation is reversible as the addition of large amounts of salt leads to a screening of charges and a break-up of the complexes. In the case of weak polyelectrolytes, the extent of interpolyelectrolyte complexation can be further controlled by varying the pH of the medium.[4]

Since the 1980s, IPECs have attracted attention due to a variety of applications, *e.g.* as environmentally friendly binders for soil and sand, or as flocculants of colloidal dispersions.[7] Their further use has been demonstrated more recently in the build-up of polyelectrolyte multilayer films or capsules *via* the layer-by-layer technique[8,9] or for the incorporation of DNA into stimuli-responsive polymer-based particles for gene delivery purposes.[10–12] Moreover, it has been shown that IPECs can be used for the immobilization of other biologically active compounds, *e.g.* proteins.[13]

If polyelectrolytes of different architectures, such as branched polymers or block co- and terpolymers, are used for IPEC formation, a variety of structures can be realized. For example, IPECs based on branched polyelectrolytes, such as star-shaped polymers or cylindrical polymer brushes, have been recently

[a]*Makromolekulare Chemie II und Bayreuther Zentrum für Kolloide und Grenzflächen, Universität Bayreuth, D-95440 Bayreuth, Germany. E-mail: axel.mueller@uni-bayreuth.de*
[b]*Department of Chemistry, M. V. Lomonosov Moscow State University, 119991 Moscow, Russia*
[c]*Institut für Organische Chemie und Makromolekulare Chemie und Jena Center for Soft Matter (JCSM), Friedrich-Schiller-Universität Jena, D-07743 Jena, Germany. E-mail: felix.schacher@uni-jena.de*

† Electronic supplementary information (ESI) available: Cryo-TEM micrographs and DLS data for micellar IPECs formed between non-crosslinked BMANaDq precursor micelles and a narrowly distributed PSSNa homopolymer, a PANa homopolymer, or a PANa-*b*-PNIPAAm diblock copolymer. Characterization of the thermo-responsive properties of the micellar IPECs with PANa-*b*-PNIPAAm. See DOI: 10.1039/c2sm26221e

reviewed.[5] Using charged block copolymers, micellar IPECs can be obtained, where the complexes form either the core[14,15] or the shell[5] of the structures. By mixing bis-hydrophilic block copolymers containing a charged and an uncharged segment with oppositely charged polyelectrolytes at stoichiometric charge ratios ($Z = 1$), water-soluble micellar IPECs are formed, which are stabilized by a corona of the hydrophilic, uncharged segments. This has been shown for either homopolymers[16–18] or diblock copolymers.[19,20] If two different (incompatible) uncharged, hydrophilic blocks build up the corona, Janus micelles can be obtained, as demonstrated by Cohen Stuart and coworkers.[21] Micellar aggregates with an IPEC shell can be realized if preformed block copolymer micelles with a charged corona are mixed with oppositely charged polyelectrolytes.[22–26] Studies on micelles with a soft polyisobutylene core and a poly(methacrylic acid) corona showed that these micelles exhibit dynamic properties even after IPEC formation.[26] Structures with a core–shell–corona architecture and an IPEC shell can also be formed by ampholytic ABC triblock terpolymers, containing both a cationic (B or C) and an anionic (C or B) segment. These then can form an intramicellar IPEC (*im*-IPEC) shell, as has been shown for both spherical[27,28] and cylindrical micelles.[29] It has been further demonstrated that these charged particles can be used as templates for the complexation with oppositely charged polyions, enabling the build-up of multi-layered structures.[30,31]

In this contribution, we demonstrate that triblock terpolymer micelles with an intramicellar IPEC (*im*-IPEC) shell are of dynamic nature and thus capable of undergoing changes in core size distribution and aggregation number during the formation of subsequent IPEC shells. The self-assembly of ampholytic polybutadiene-*block*-poly(sodium methacrylate)-*block*-poly{2-[(methacryloyloxy)ethyl]trimethylammonium methylsulfate} (PB-*b*-PMANa-*b*-PDMAEMAq) triblock terpolymers in aqueous media at high pH leads to stimuli-responsive multi-compartment micelles with a soft PB core, a PMANa/PDMAEMAq *im*-IPEC shell, and a positively charged PDMAEMAq corona. The latter is formed as the degree of polymerization (DP) of PDMAEMAq is higher than that of the middle block, PMANa. Upon electrostatic co-assembly with negatively charged homopolymers (PSSNa) at different charge ratios, further IPEC formation occurs. We show that during the formation of this shell the size of the PB core and, thus, the aggregation number of the micelles changes significantly. Similar observations have already been made earlier[28,31] and we attribute this to the low glass transition temperature ($T_g \sim -15$ °C) of the PB block with a predominant 1,2-microstructure.[32] If now the PB core is crosslinked prior to IPEC formation, such dynamics can be suppressed and uniform, multi-layered micellar IPECs can be prepared. Crosslinking was performed by introducing a UV photo-initiator, Lucirin® TPO, into the micellar core during self-assembly of the PB-*b*-PMANa-*b*-PDMAEMAq triblock terpolymers. We also show that by using PANa-*b*-PNIPAAm diblock copolymers for electrostatic co-assembly, micellar IPECs with a PNIPAAm corona can be formed and that these multi-layered structures exhibit thermo-responsive properties. For the characterization of all micellar structures, a combination of cryogenic transmission electron microscopy (cryo-TEM) and dynamic light scattering (DLS) was used.

Experimental part

Synthesis

Materials. Poly(sodium 4-styrenesulfonate) (PSSNa, M_w = 70 000 g mol^{-1}, PDI ~2 (determined by size exclusion chromatography (SEC) in H_2O with 30% MeOH, 0.1 M NaN_3, and 0.01 M NaH_2PO_4 calibrated with poly(ethylene oxide) standards)) and poly(acrylic acid) (PAA, $M_w = 1.25 \times 10^6$ g mol^{-1}) were purchased from Aldrich and used as received. Narrowly distributed PSSNa ($M_n = 20\,000$ g mol^{-1}, PDI = 1.02) was purchased as a molecular weight standard from Polymer Standard Service PSS. Lucirin® TPO (2,4,6-trimethylbenzoylphosphine oxide), the UV photoinitiator, was kindly provided by BASF and used as received. All solvents were purchased in p.a. grade and used without further purification. All aqueous solutions were prepared either from Millipore water or pH 10 buffer solutions (VWR, AVS Titrinorm, boric acid buffer) with an ionic strength of *ca.* 0.05 M. Water was purified with a Milli-Q water purification system by Millipore. For all dialysis steps in this work, membranes of regenerated cellulose (Spectra/Por, Roth) with a molecular weight cut-off (MWCO) of 3500 g mol^{-1} were used. Prior to use, the tubes were immersed in de-ionized water to open the pores.

Synthesis of PB-*b*-PMANa-*b*-PDMAEMAq triblock terpolymers. The polybutadiene-*block*-poly(*tert*-butyl methacrylate)-*block*-poly(2-(dimethylamino)ethyl methacrylate) (PB-*b*-P*t*BMA-*b*-PDMAEMA) terpolymer was synthesized *via* sequential living anionic polymerization in THF and modified to polybutadiene-*block*-poly(sodium methacrylate)-*block*-poly{2-[(methacryloyloxy)ethyl]trimethylammonium methylsulfate} (PB-*b*-PMANa-*b*-PDMAEMAq, BMANaDq). We obtained the triblock terpolymer $B_{800}MANa_{200}Dq_{285}$ (subscripts denote the degrees of polymerization of the corresponding blocks, M_n = 110 000 g mol^{-1}, PDI = 1.10). Details about the synthetic procedure and a comprehensive investigation of the PB-*b*-PMANa-*b*-PDMAEMAq triblock terpolymers in solution can be found elsewhere.[28]

Synthesis of PAA-*b*-PNIPAAm diblock copolymers. The poly(acrylic acid)-*block*-poly(*N*-isopropylacrylamide) (PAA-*b*-PNIPAAm) diblock copolymer, $AA_{27}NIPAAm_{150}$ (M_n = 18 900 g mol^{-1}, PDI = 1.08), was synthesized *via* RAFT polymerization. The synthesis and characterization have been reported elsewhere.[33]

Preparation of PB-*b*-PMANa-*b*-PDMAEMAq micellar solutions. After modification of the terpolymer to PB-*b*-PMANa-*b*-PDMAEMAq (BMANaDq), a micellar stock solution ($c = 0.5$ g L^{-1}) was prepared *via* dialysis against pH 10 buffer solution.

Crosslinking of the micellar aggregates. Crosslinking of the PB core in BMANaDq micelles was performed directly after the quaternization reaction in a dioxane/water mixture (1 : 1, v/v) by the addition of a UV photoinitiator, Lucirin® TPO (2,4,6-trimethylbenzoylphosphine oxide, BASF). 25 wt% Lucirin® TPO, calculated according to the weight fraction of polybutadiene, were added to the polymer solution ($c \sim 0.5$ g L^{-1}) under the exclusion of light. After stirring for 1 hour, the mixture was dialyzed against pH 10 buffer solution. The dialysis was carried

out in the dark to prevent decomposition of the UV photoinitiator. Afterwards, the micellar solution was irradiated with a UV lamp (Hoehnle UVAHAND 250 GS, equipped with a quartz glass filter) under continuous stirring for 30 min.

Preparation of interpolyelectrolyte complexes. PSSNa, PAA, and the PAA-*b*-PNIPAAm diblock copolymer were dissolved in pH 10 buffer solution (c = 0.5 g L^{-1}). Afterwards, the corresponding volumes to reach a certain $Z_{-/+}$ value (overall ratio of negative to positive charges, where the positive charges represent PDMAEMAq units, which are not involved in intramicellar IPEC formation, see also eqn (1)) were added to a micellar solution of BMANaDq or core-crosslinked BMANaDq (xBMANaDq) in pH 10 buffer (c = 0.2 or 0.25 g L^{-1}) in small glass vials and stirred at room temperature. The final micellar concentrations were in the range of 0.2–0.3 g L^{-1}. In general, measurements on the IPECs were performed after one week of continuous stirring.

Characterization

Dynamic light scattering (DLS). DLS measurements were performed on an ALV DLS/SLS-SP 5022F compact goniometer system with an ALV 5000/E cross-correlator and a He–Ne laser (λ = 632.8 nm). The measurements were carried out in cylindrical scattering cells (d = 10 mm) at an angle of 90° and a temperature of 20 °C. Prior to the measurements, the sample solutions were filtered using nylon filters (Magna, Roth) with a pore size of 5 μm. For temperature-dependent measurements, the temperature of the decaline bath of the instrument was controlled using a LAUDA Proline RP 845 thermostat. The temperature was increased in steps of 2 K followed by an equilibration time of 5 min prior to each measurement. The CONTIN algorithm was applied to analyze the obtained correlation functions. Apparent hydrodynamic radii were calculated according to the Stokes–Einstein equation. Apparent polydispersities for the aggregates in solution were determined from unimodal peaks *via* the cumulant analysis.

Cryogenic transmission electron microscopy (cryo-TEM). For cryo-TEM studies, a drop (~2 μL) of the aqueous micellar solution ($c \sim$ 0.5 g L^{-1}) was placed on a lacey carbon-coated copper TEM grid (200 mesh, Science Services), where most of the liquid was removed with blotting paper, leaving a thin film stretched over the grid holes. The specimens were shock vitrified by rapid immersion into liquid ethane in a temperature-controlled freezing unit (Zeiss Cryobox, Zeiss NTS GmbH) and cooled to approximately 90 K. The temperature was monitored and kept constant in the chamber during all of the preparation steps. After freezing the specimens, they were inserted into a cryo-transfer holder (CT3500, Gatan) and transferred to a Zeiss EM922 OMEGA EFTEM instrument. Examinations were carried out at temperatures around 90 K. The microscope was operated at an acceleration voltage of 200 kV. Zero-loss filtered images (ΔE = 0 eV) were taken under reduced dose conditions. All images were registered digitally by a bottom-mounted CCD camera system (Ultrascan 1000, Gatan), combined, and processed with a digital imaging processing system (Gatan Digital Micrograph 3.9 for GMS 1.4).

Flow tube reactor. IPEC formation with ultrafast mixing of the components was carried out in a specially designed flow tube reactor containing a mixing jet with a mixing time of <1 ms.[34,35] For this experiment, a PSSNa solution was prepared in pH 10 buffer and mixed with BMANaDq micelles at a ratio of $Z_{-/+} = 1$. As the components could only be mixed in the flow tube reactor in equal volumes, the concentrations of both solutions were adjusted to reach $Z_{-/+} = 1$. Therefore, the BMANaDq micelles were used at a concentration of 0.5 g L^{-1} and PSSNa at 0.08 g L^{-1}.

Turbidity measurements. Turbidity measurements were performed using a Metrohm Titrando 809 system equipped with a Spectrosense turbidity sensor (λ = 523 nm, Metrohm) and a Pt 1000 temperature sensor. The measurements were carried out in a thermostatted glass chamber. The temperature program (0.15 K min^{-1}) was run by a LAUDA RE 306 thermostat. The turbidity measurements were performed with freshly prepared solutions at a concentration of approximately 0.3 g L^{-1} for the micellar IPECs and 0.5 g L^{-1} for the PANa-*b*-PNIPAAm diblock copolymer. All measurements were conducted in buffer solutions to keep the pH constant over the entire temperature range. The solutions were degassed by applying vacuum (50–100 mbar) for 15 min at room temperature to minimize bubble formation during heating. Prior to the measurements, the sample solutions were filtered using nylon filters (Magna, Roth) with a pore size of 5 μm.

Results and discussion

Core–shell–corona micelles from PB-*b*-PMANa-*b*-PDMAEMAq

Recently, we reported on the self-assembly of ampholytic polybutadiene-*block*-poly(sodium methacrylate)-*block*-poly{2-[(methacryloyloxy)ethyl]trimethylammonium methylsulfate} $B_{800}MANa_{200}Dq_{285}$ (M_n = 110 000 g mol^{-1}, PDI = 1.10) triblock terpolymers in aqueous media.[28] The subscripts denote the degrees of polymerization of the corresponding blocks. For simplicity reasons, the terpolymer will be denoted as BMANaDq throughout the manuscript. The chemical structure of the terpolymer is shown in Fig. 1A. In an aqueous solution at high pH, the terpolymer forms core–shell–corona micelles with a soft PB core, an intramicellar interpolyelectrolyte complex (*im*-IPEC) shell formed between negatively charged PMANa and positively charged PDMAEMAq, and a positively charged corona of excess PDMAEMAq (DP_n(PDMAEMAq) > DP_n(PMANa)). This renders micelles with a positive corona charge. A cryo-TEM micrograph of the micelles at pH 10 and the proposed solution structure are shown in Fig. 1B and C. The inset in Fig. 1B depicts two adjacent micelles connected by a hydrophobic bridge (dark grey), possibly showing the fusion of the two structures. At pH 10, the micelles exhibit a hydrodynamic radius of $\langle R_h \rangle_z \sim$ 107 nm, as determined *via* dynamic light scattering (DLS). We showed that the micelles are able to react on changes in pH and salinity. Here, these structures will be used as "precursor" micelles for the complexation with different oppositely charged polyelectrolytes and the consequent build-up of IPEC layers.

Interpolyelectrolyte complex formation

We started by mixing a commercially available negatively charged strong polyelectrolyte, poly(sodium 4-styrenesulfonate) (PSSNa), with positively charged BMANaDq micelles. In that

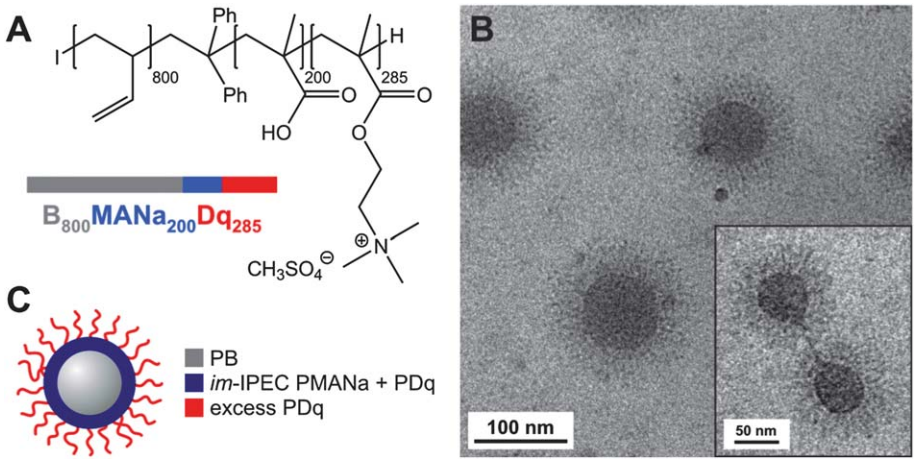

Fig. 1 Structure and composition of the BMANaDq triblock terpolymer (A); cryo-TEM micrograph of BMANaDq precursor micelles in aqueous solution ($c = 0.5$ g L^{-1}) at pH 10 (B), the inset shows hydrophobic bridges between two adjacent micelles; the proposed core–shell–corona structure at pH 10 (C).[28]

way, one can expect an additional IPEC shell to be formed through the complexation of PSSNa with PDMAEMAq as the corona-forming block. The whole process is depicted in Scheme 1. In all cases, IPEC formation is performed at high pH (pH 10), leading to complete ionization of PMAA. Different charge ratios of polyanion to polycation are used, represented by the $Z_{-/+}$ value. $Z_{-/+}$ refers to the number of anionic PSSNa (or later PANa) units added to the micellar solution divided by the number of free (not involved in *im*-IPEC formation) cationic PDMAEMAq units present (eqn (1)).

$$Z_{-/+} = \frac{n_{\mathrm{PSSNa/PANa}}}{n_{\mathrm{PDq}} - n_{\mathrm{PMANa}}} \quad (1)$$

We have recently shown that hydrophobic bridges between individual BMANaDq micelles (Fig. 1B, inset)[28] or polybutadiene-*block*-poly(1-methyl-2-vinyl pyridinium)-*block*-poly(sodium methacrylate) (BVqMANa) micelles with a rather thin corona can be formed.[31] This was attributed to the low glass transition temperature (T_g) of the core-forming PB block and the lower density of the *im*-IPEC between PMANa and PDMAEMAq, as compared to the earlier work on PMANa and P2VPq.[31] We therefore now also crosslink the PB core using a UV photoinitiator and compare the micellar structure and any additional IPEC shells formed between both core states (crosslinked and non-crosslinked). The strategy involving crosslinked micelles, xBMANaDq, is depicted in Scheme 1.

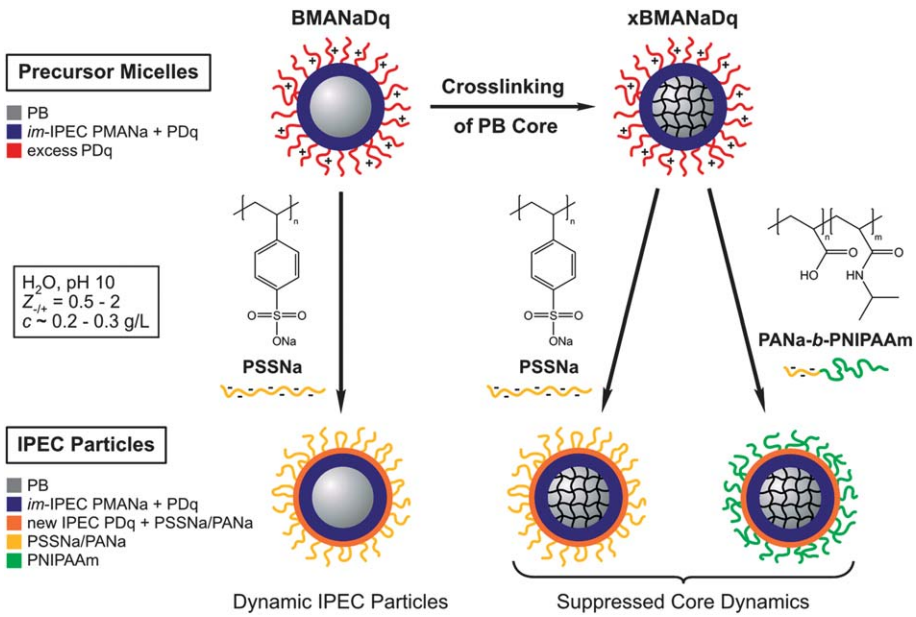

Scheme 1 Formation of various micellar IPECs from positively charged BMANaDq precursor micelles and negatively charged PSSNa homopolymers; by crosslinking of the PB core of the precursor micelles, the dynamics of the micellar core are suppressed; and complexation with bis-hydrophilic PANa-*b*-PNIPAAm diblock copolymers renders thermo-responsive micellar IPECs with a water-soluble PNIPAAm corona.

Not only homopolymers, but also diblock copolymers can be used for the formation of the additional IPEC shell. We have already shown this for the complexation of negatively charged micelles with poly(ethylene oxide)-*block*-poly(1-methyl-2-vinyl pyridinium) (PEO-*b*-P2VPq)[30] and PEO-*b*-PDMAEMAq[31] diblock copolymers. Here, we used bis-hydrophilic poly(sodium acrylate)-*block*-poly(*N*-isopropylacrylamide) (PANa-*b*-PNIPAAm). PNIPAAm is well-studied and shows temperature-dependent solubility in aqueous solution (LCST = 32 °C).[36] Complexation between crosslinked xBMANaDq micelles and PANa-*b*-PNIPAAm should also lead to the formation of an additional IPEC shell of PANa and PDMAEMAq, but the particles will be surrounded by a hydrophilic PNIPAAm corona. In this case, even for $Z_{-/+} = 1$, the micellar IPECs are expected to remain water-soluble. The use of diblock copolymers for the complexation provides the opportunity to introduce further functionality to IPEC particles. Here, our aim was to transfer the thermo-responsive properties of the PNIPAAm block to the IPEC structures.

For all complexation reactions, BMANaDq or core-crosslinked xBMANaDq precursor micelles were used at a concentration of 0.20 or 0.25 g L^{-1} in pH 10 buffer solutions. The targeted amounts of homo- or diblock copolymers were added at a concentration of 0.5 g L^{-1}, using identical pH 10 buffer solutions. The polyanions were added under vigorous stirring, and the resulting micellar IPECs were examined after approximately one week of continuous stirring.

Complexation of BMANaDq micelles with PSSNa

We used commercially available PSSNa as a strong anionic polyelectrolyte with a molecular weight of $M_w = 70\,000$ g mol^{-1}, corresponding to an average of 170 repeating units. The precursor micelles were mixed with PSSNa at different $Z_{-/+}$ ratios (Scheme 1) and the size of the IPECs was determined by DLS measurements. The corresponding CONTIN plots are shown in Fig. 2. Initially, the BMANaDq precursor micelles exhibit a hydrodynamic radius of $\langle R_h \rangle_z = 107$ nm. After the addition of PSSNa at $Z_{-/+} = 0.5$, 1, and 2, slight changes in hydrodynamic radius indicate a successful complexation: at $Z_{-/+} = 0.5$, the formed particles ($\langle R_h \rangle_z = 101$ nm) are smaller, which can be attributed to a partial collapse of the PDMAEMAq corona chains upon interaction with PSSNa. Further, the micellar IPECs remain stable in aqueous environment, which can be explained by the remaining positive net charge. At $Z_{-/+} \geq 1$, the size of the aggregates increases to $\langle R_h \rangle_z = 111$ nm at $Z_{-/+} = 1$ and $\langle R_h \rangle_z = 114$ nm at $Z_{-/+} = 2$. The particles remain soluble even at $Z_{-/+} = 1$, and only a slight broadening of the size distribution according to DLS can be observed, indicating changes induced *via* further IPEC formation. For all $Z_{-/+}$ values, the distributions are significantly broader as compared to the precursor micelles.

To further investigate the structure of the micellar IPECs, we performed cryogenic transmission electron microscopy (cryo-TEM) experiments at different $Z_{-/+}$ ratios (Fig. 3B–D). In all cases, predominantly spherical micellar IPECs with a grey PB core surrounded by a thick, fuzzy IPEC shell are visible. Compared to the "bare" (precursor) BMANaDq micelles (Fig. 3A), the thickness of the IPEC shell slightly increased,

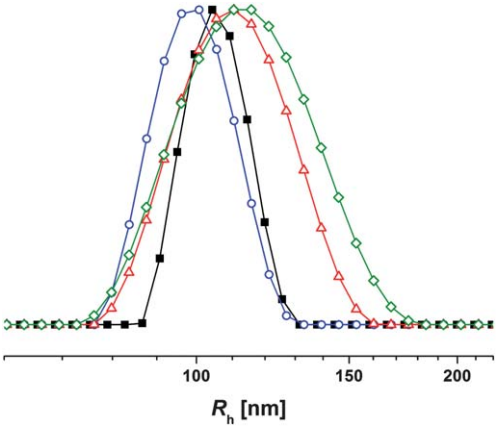

Fig. 2 Intensity-weighted DLS CONTIN plots for BMANaDq precursor micelles in aqueous solution at pH 10 (-■-, $\langle R_h \rangle_z = 107$ nm, PDI = 0.06) and micellar IPECs with PSSNa at $Z_{-/+} = 0.5$ (-○-, $\langle R_h \rangle_z = 101$ nm, PDI = 0.08), $Z_{-/+} = 1$ (-△-, $\langle R_h \rangle_z = 111$ nm, PDI = 0.10), and $Z_{-/+} = 2$ (-◇-, $\langle R_h \rangle_z = 114$ nm, PDI = 0.11).

hinting towards a successful complexation with PSSNa. However, the two individual IPEC layers (the "old" *im*-IPEC shell and the "new" IPEC shell formed between PDMAEMAq and PSSNa) cannot be distinguished, as both seem to exhibit similar electron densities. In the case of $Z_{-/+} = 1$, an average thickness of the IPEC shell of 40 nm was found, which is larger than the shell thickness for the former *im*-IPEC (31 nm). A detailed analysis of the shell thickness at different $Z_{-/+}$ ratios was not possible due to the rather low electron contrast of the IPEC shell.

Upon IPEC formation, the polydispersity of the micellar IPECs dramatically increases, when compared to the original BMANaDq structures (Fig. 3A). This is in accordance with the DLS studies described above (Fig. 2). To obtain further quantitative evidence of the broadening of the micellar size distributions, several cryo-TEM micrographs were subjected to a detailed image analysis determining the core radius of the micelles. The core radius distributions for the precursor micelles and the micellar IPECs at $Z_{-/+} = 1$, obtained from approximately 100 to 250 (spherical) micelles for each sample, are displayed as histograms fitted using a Gaussian distribution in Fig. 3E. The number-average core radii, $\langle R_{core} \rangle_n$, are listed together with the corresponding standard deviations, σ, in Table 1. Comparing the histograms before and after IPEC formation, a significant broadening of the core radius distribution upon complexation can be observed. In particular, the fraction of micelles with a rather small radius increases. Consequently, the average core radius of the IPECs at $Z_{-/+} = 1$ ($\langle R_{core} \rangle_n = 26$ nm) is lower than that of the precursor micelles ($\langle R_{core} \rangle_n = 36$ nm). Apparently, a smaller core size and consequently a smaller aggregation number are favored after complexation and increase of the thickness of the hydrophobic IPEC shell around the PB core.

These changes in core size strongly indicate a dynamic behavior of the BMANaDq precursor micelles during complexation. Since exchange of unimers with a long PB block is impossible, we propose micellar fusion/fission processes as the mechanism. This is enabled by the low glass transition

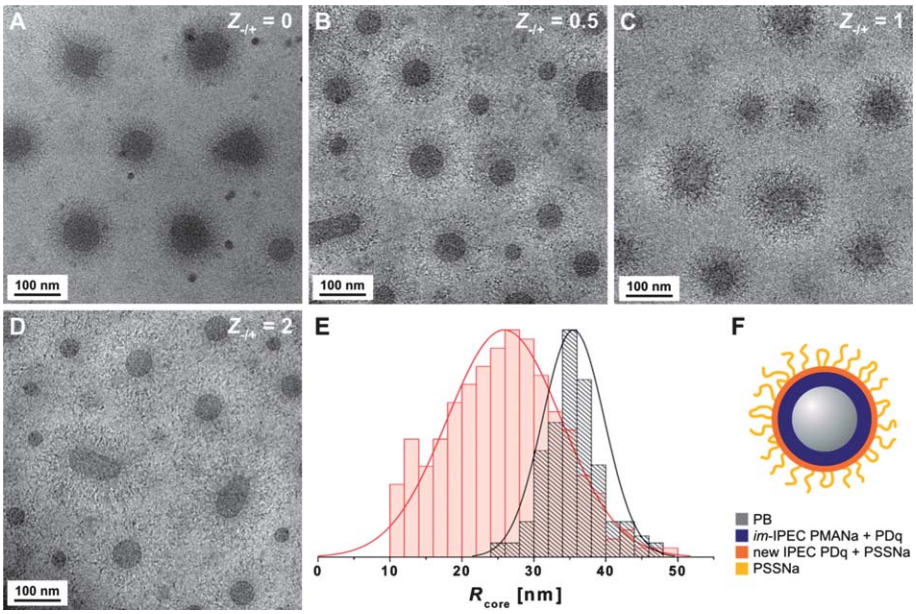

Fig. 3 Cryo-TEM micrographs of BMANaDq precursor micelles (A, $Z_{-/+} = 0$; reproduced with permission from ref. 28; Copyright 2011, The Royal Society of Chemistry) and micellar IPECs from BMANaDq and PSSNa in aqueous solution at pH 10 at different $Z_{-/+}$ ratios; $Z_{-/+} = 0.5$ (B), $Z_{-/+} = 1$ (C), and $Z_{-/+} = 2$ (D); core radius distributions for BMANaDq precursor micelles (black, $\langle R_{core} \rangle_n = 36$ nm, $\sigma(R_{core}) = 4$ nm) and micellar IPECs from BMANaDq and PSSNa at $Z_{-/+} = 1$ (red, $\langle R_{core} \rangle_n = 26$ nm, $\sigma(R_{core}) = 8$ nm) (E); proposed solution structure of the micellar IPECs at $Z_{-/+} > 1$ (F).

temperature of the core-forming block, PB, and relatively low electrostatic repulsion between the precursor micelles. Recently, Lodge *et al.* confirmed that the T_g of polystyrene (PS) in block copolymer micelles with a PS core is comparable to the T_g of the bulk material.[37] Thus, we can assume that the T_g of the core-forming PB for BMANaDq micelles is below room temperature. Further, we operate at rather low salt concentrations (*ca.* 50 mM). This is in accordance with earlier studies on the solution properties of BMANaDq micelles in response to various external stimuli, such as pH, temperature, or salinity.[28] Another observation supporting this hypothesis is the presence of hydrophobic bridges between different PB cores of adjacent micelles (Fig. 1B, inset). Such bridges between PB cores have previously been observed in micellar systems of other ABC (linear and miktoarm star) terpolymers in water.[31,38]

Cryo-TEM micrographs of micellar IPECs at different $Z_{-/+}$ ratios are depicted in Fig. 3B–D ($Z_{-/+} = 0.5$, 1, and 2, respectively). For $Z_{-/+} = 0.5$ and 2, some elongated micellar structures with similar width but a significantly increased length are also observed. This is another indication for the occurrence of micellar fusion processes. Bearing in mind that hydrophobic bridges were already present between individual BMANaDq micelles, one single PSSNa chain might be incorporated into the IPEC shell of two precursor micelles in such cases.

More remarkably, the particles remain water-soluble at $Z_{-/+} \geq 1$, although all PDMAEMAq corona segments should be complexed with PSSNa. For $Z_{-/+} > 1$, an explanation could be that a fraction of the excess PSSNa chains is rather loosely associated, forming non-equilibrium structures analogous to "loops" and "trails", known from the adsorption of polyelectrolytes onto oppositely charged surfaces.[39,40] This would lead to a charge overcompensation of the structures and a net negative charge. This effect plays a crucial role in the formation of polyelectrolyte multilayers and capsules *via* the layer-by-layer technique, where charge inversion enables the consecutive adsorption of alternating layers of polyanions and polycations.[8,41,42] For micellar systems, charge overcompensation has already been shown to operate for the complexation of PSSNa with protonated polystyrene-*block*-poly(2-vinylpyridine) (PS-*b*-P2VPH$^+$) micelles in water at low pH.[43] This would explain the observed colloidal stability of the micellar IPECs in aqueous solution in our case. The proposed solution structure of the micellar IPECs at $Z_{-/+} > 1$ is depicted in Fig. 3F.

Table 1 Average hydrodynamic radii $\langle R_h \rangle_z$ and average core radii $\langle R_{core} \rangle_n$ with standard deviations σ of BMANaDq and core-crosslinked xBMANaDq micelles and micellar IPECs formed from both types of precursor micelles and PSSNa at $Z_{-/+} = 1$

	$\langle R_h \rangle_z{}^a$ [nm]	$\sigma(R_h)^a$ [nm]	$\langle R_{core} \rangle_n{}^b$ [nm]	$\sigma(R_{core})^b$ [nm]
BMANaDq	107	6	36	4
BMANaDq + PSSNa	111	11	26	8
xBMANaDq	107	6	33	4
xBMANaDq + PSSNa	124	7	34	4

[a] Determined by DLS. [b] Determined by image analysis of cryo-TEM micrographs.

An important point that has to be discussed is the possible substitution of $PMAA^-$ segments in the *im*-IPEC shell of the initial BMANaDq micelles by added PSS^- chains. The polyion exchange and substitution reactions within IPECs have been extensively studied by Kabanovs and coworkers.[44–47] They showed that the kinetics and the position of the equilibrium substantially depend on the chemical nature of the polyions. In particular, polysulfonates (*e.g.* PSSNa) generally replace polycarboxylates (*e.g.*, PMANa) in IPECs containing polyamines as the polycation.[4,48] In addition to Coulombic attraction, the driving force for this substitution is a specific affinity of the sulfonate groups for protonated or quaternary amino groups. This strong selective binding of polycations with sulfonate-containing polyanions has also been shown for polyelectrolyte multilayers.[49] Schlenoff and coworkers reported a significant difference in the free energy of association of a quaternized amine group with a sulfonate group compared to a carboxylate group.[50,51] A different study by the Kabanov group showed that the direction of substitution reactions in IPECs strongly depends on the chain length of the competing polyion.[52] Due to entropic reasons, the substitution reaction is favored by an increasing degree of polymerization of the competitive polyanion. In our case, however, the average length of the PSSNa chains (DP_n = 170) is comparable to that of the PMANa chains (DP_n = 200). In addition, the kinetics of such polyion reactions are drastically affected by the ionic strength. They have been shown to be absent in salt-free solutions.[45] With increasing salt concentration some of the ionic bonds dissociate, resulting in defects in a system of interpolymer salt bonds, accelerating any polyion substitution.

In summary, these earlier findings do suggest that the replacement of PMA^- in the *im*-IPEC shell through PSS^- is probable in our case, especially at high $Z_{-/+}$ values. This would lead to rearrangements within the micellar shell and to the release of some MA^- groups from the *im*-IPEC by substitution with added PSSNa. We assume that this exchange, however, is incomplete, as for the used $Z_{-/+}$ values the amount of added PSSNa is not sufficient for a complete substitution. Additionally, in our system the interaction of PMANa with PDMAEMAq might be enhanced, since PMANa as the middle block is covalently bound to PDMAEMAq, hindering rearrangement processes within the *im*-IPEC shell. Consequently, the released MA^- groups might remain as MANa groups within the IPEC shell, forming a ternary mixed shell of PMANa/PSSNa/PDMAEMAq, in which free ionic groups of PMAA are present. These charges then are only compensated by Na counterions and may consequently impart a certain hydrophilicity to the IPEC shell, rendering it loose and rather swollen. This also would improve the solubility of these structures in water even at $Z_{-/+} = 1$, where the overcharging effect might be negligible. Additionally, this partial substitution of PMAA by PSS would change the actual $Z_{-/+}$ ratios.

The molecular weight distribution of the PSSNa homopolymer might influence the size distribution of the micellar IPECs. So far, commercially available PSSNa with a broad molecular weight distribution was used. Therefore, we also used narrowly distributed PSSNa (M_n = 20 000 g mol^{-1}, DP_n = 100, PDI = 1.02). IPECs were prepared at pH 10 and $Z_{-/+} = 1$ and cryo-TEM investigations (Fig. S1† ESI) show that here also the micellar core size distribution broadened in a similar way. In conclusion, the polydispersity of the polyanion used for complexation seems to be negligible for our system.

It might be argued that the polydispersity of the micellar IPECs is due to the mixing of reactants being slow compared to IPEC formation, as it has been shown that this process occurs within less than several ms.[45] We therefore performed IPEC formation using ultrafast mixing of the components in a flow tube reactor and compared the results with those obtained for conventional mixing *via* magnetic stirring (Fig. 4). The setup contains a mixing jet that allows for mixing times lower than 1 ms.[34,35] The precursor micelles and PSSNa solutions were prepared in pH 10 buffer and mixed at a ratio of $Z_{-/+} = 1$. A cryo-TEM micrograph of the resulting structures is shown in Fig. 4B. Again, the polydispersity of the micelles increased upon IPEC formation. The micellar core size distributions for Fig. 4A and B broadened comparably, both after slow and fast mixing. We therefore conclude that the influence of the mixing rate in our case is negligible, at least with regard to the IPEC formation with PSSNa. Therefore, all following complexation experiments have been carried out by conventional, "slow" mixing as described before.

Core crosslinking of BMANaDq precursor micelles

Several aspects, *e.g.* the occurrence of hydrophobic bridges or deformations and size changes of the micellar core, point towards a dynamic behavior of BMANaDq micelles. We therefore crosslinked the PB core using a UV photoinitiator, Lucirin® TPO. This should suppress any segmental dynamics and also micellar fusion/fission processes. 25 wt% Lucirin® TPO (calculated according to the PB content of the triblock terpolymer) were added to a solution of the BMANaDq terpolymer in a mixture of dioxane and water (1 : 1, v/v). The solution was dialyzed against pH 10 buffer (in the dark, to avoid any decomposition of the UV photoinitiator) to trigger the formation of micelles and the anticipated incorporation of the photoinitiator into the hydrophobic PB core of the micelles. After dialysis, the micellar core was crosslinked *via* UV irradiation for 30 minutes. The photoinitiator, Lucirin® TPO, has already been used to crosslink PB in micellar aggregates of PB-*b*-P2VP in solution[53] as well as in different PB-containing terpolymers in the bulk.[29,32]

The DLS CONTIN plots of the core-crosslinked xBMANaDq micelles in comparison to the non-crosslinked analogues are shown in Fig. 5. The size of the BMANaDq micelles did not

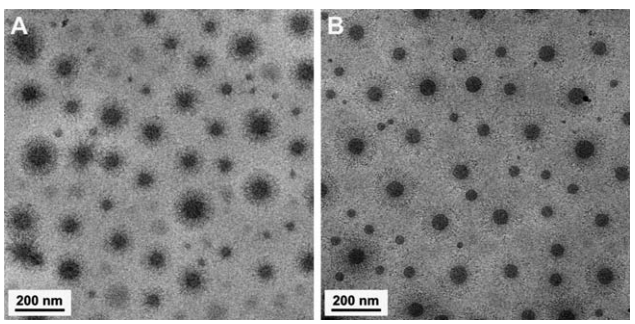

Fig. 4 Cryo-TEM micrographs of micellar IPECs from BMANaDq precursor micelles and PSSNa in aqueous solution at pH 10 and $Z_{-/+} = 1$ prepared by conventional (A) and ultrafast mixing in a flow tube reactor (B).

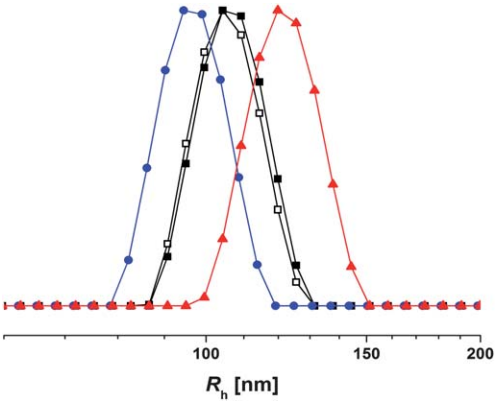

Fig. 5 Intensity-weighted DLS CONTIN plots for BMANaDq precursor micelles before crosslinking in aqueous solution at pH 10 (-□-, $\langle R_h \rangle_z = 107$ nm, PDI = 0.06), after crosslinking in aqueous solution at pH 10 (-■-, $\langle R_h \rangle_z = 107$ nm, PDI = 0.06), after crosslinking in dioxane (-●-, $\langle R_h \rangle_z = 99$ nm, PDI = 0.06), and micellar IPECs from crosslinked xBMANaDq precursor micelles and PSSNa at $Z_{-/+} = 1$ (-▲-, $\langle R_h \rangle_z = 124$ nm, PDI = 0.06).

change upon crosslinking. Before and after crosslinking, the micelles exhibit a hydrodynamic radius of $\langle R_h \rangle_z = 107$ nm. To prove the successful crosslinking of the PB core, the micellar solution was dialyzed from pH 10 buffer against dioxane. The corresponding DLS CONTIN plot shows that micellar aggregates with a hydrodynamic radius of $\langle R_h \rangle_z = 99$ nm are still present. The smaller hydrodynamic radius in dioxane is explained by a partial collapse of the positively charged PDMAEMAq corona. The existence of micelles in dioxane indicates a successful crosslinking of the PB core.

A cryo-TEM micrograph of the crosslinked xBMANaDq micelles is shown in Fig. 6A. The micelles are of uniform size and still exhibit the core–shell–corona structure as observed before crosslinking (Fig. 1B and 3A). Also here, we analyzed the cryo-TEM micrographs quantitatively to estimate the radius of the PB core. Approximately 100 micelles were measured for each sample to calculate the average radii. For the crosslinked xBMANaDq micelles, an average radius of the micellar core of $\langle R_{core} \rangle_n = 33$ nm was obtained. This is very close to the radius of the non-crosslinked BMANaDq micelles of $\langle R_{core} \rangle_n = 36$ nm (Table 1).

Complexation of core-crosslinked xBMANaDq micelles with PSSNa

To confirm our assumption that core crosslinking suppresses any changes in core size, the xBMANaDq micelles were then mixed with PSSNa (Scheme 1). Micellar IPECs with PSSNa were prepared in pH 10 buffer solution at $Z_{-/+} = 1$ applying the same procedure as described before. DLS CONTIN plots of the obtained micellar IPECs are shown in Fig. 5, giving a hydrodynamic radius of $\langle R_h \rangle_z = 124$ nm. The fact that the overall size of the micellar IPECs increases despite the formation of another IPEC shell supports our proposed structure with at least partial substitution of PMANa in the *im*-IPEC with PSSNa and, hence, the existence of a swollen and partially hydrophilic IPEC shell. The polydispersity of the IPECs is in the same range as that of the precursor micelles and did not increase upon complexation. This is already an indication for the suppression of any rearrangements in the micellar core. Further, the size of the core-crosslinked micellar IPECs ($\langle R_h \rangle_z = 124$ nm) is even slightly larger than that of the IPECs obtained earlier without core crosslinking at $Z_{-/+} = 1$ ($\langle R_h \rangle_z = 111$ nm). In that case, an additional significant broadening of the micellar size distribution was observed.

A cryo-TEM micrograph of the core-crosslinked micellar IPECs with PSSNa at $Z_{-/+} = 1$ is shown in Fig. 6B. Uniform micellar IPECs can be seen. In contrast to the non-crosslinked particles (Fig. 3C), here the core size distribution did not seem to change upon IPEC formation. The average core radii of the xBMANaDq micelles and the corresponding micellar IPECs were determined *via* image analysis of the cryo-TEM micrographs by measuring approximately 100 micelles for each sample. The respective core radius distributions are displayed as histograms with a Gaussian fit in Fig. 6C. As can be seen, the average core radius for the xBMANaDq micelles ($\langle R_{core} \rangle_n = 33$ nm) and for the micellar IPECs ($\langle R_{core} \rangle_n = 34$ nm) remained constant (Table 1). We believe that this convincingly demonstrates that core crosslinking suppresses any changes in core size or aggregation number upon further IPEC formation. Obviously, the lack of mobility of the PB core after crosslinking inhibits any fusion/fission processes to which we attributed the observed dynamics. Moreover, the crosslinking procedure presents a facile way to generate uniform and well-defined multi-layered micellar IPECs.

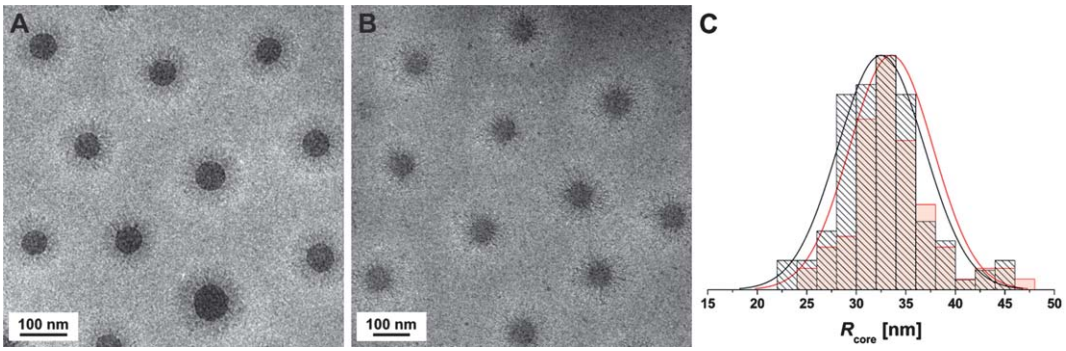

Fig. 6 Cryo-TEM micrographs of core-crosslinked xBMANaDq precursor micelles in aqueous solution at pH 10 (A); and micellar IPECs from xBMANaDq and PSSNa at $Z_{-/+} = 1$ (B); core radius distributions for xBMANaDq precursor micelles (black, $\langle R_{core} \rangle_n = 33$ nm, $\sigma(R_{core}) = 4$ nm) and micellar IPECs from xBMANaDq and PSSNa at $Z_{-/+} = 1$ (red, $\langle R_{core} \rangle_n = 34$ nm, $\sigma(R_{core}) = 4$ nm) (C).

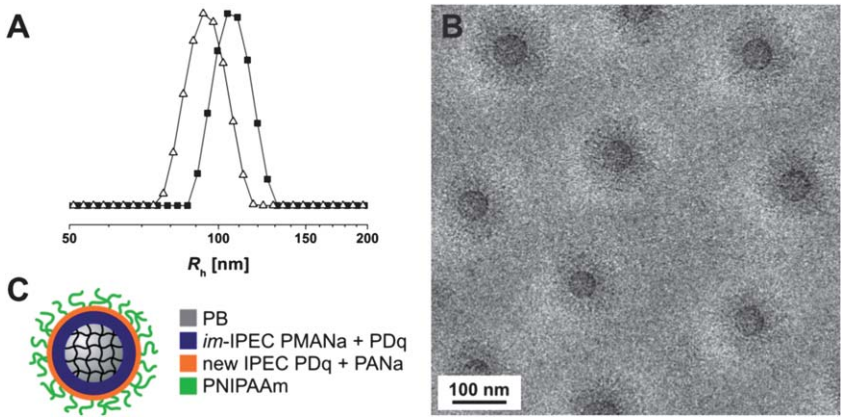

Fig. 7 Intensity-weighted DLS CONTIN plots for core-crosslinked xBMANaDq precursor micelles in aqueous solution at pH 10 (-■-, $\langle R_h \rangle_z$ = 107 nm, PDI = 0.06) and micellar IPECs with $ANa_{27}NIPAAm_{150}$ at $Z_{-/+} = 1$ (-△-, $\langle R_h \rangle_z$ = 99 nm, PDI = 0.08) (A); cryo-TEM micrograph of micellar IPECs from xBMANaDq and $ANa_{27}NIPAAm_{150}$ at $Z_{-/+} = 1$ (B); and proposed solution structure of the micellar IPECs (C).

Complexation of core-crosslinked xBMANaDq micelles with bis-hydrophilic PANa-*b*-PNIPAAm diblock copolymers

After the successful formation of well-defined micellar IPECs with PSSNa homopolymers, our aim was to introduce further functionality into the precursor micelles *via* IPEC formation. For this purpose, poly(sodium acrylate)-*block*-poly(*N*-isopropylacrylamide (PANa-*b*-PNIPAAm) diblock copolymers were used for complexation to transfer the thermo-responsive properties of the PNIPAAm segment to the micellar IPECs. Prior to IPEC formation with PANa-*b*-PNIPAAm, comparable experiments were carried out using a PANa homopolymer (Fig. S2, ESI†). The bis-hydrophilic PANa-*b*-PNIPAAm diblock copolymer, $ANa_{27}NIPAAm_{150}$, exhibits thermo-responsive properties, owing to the LCST behavior of the PNIPAAm block (LCST of PNIPAAm = 32 °C).[36] Again, IPEC formation takes place at pH 10, where full ionization of the PAA segments can be expected. The resulting micellar IPECs should remain water-soluble, even at $Z_{-/+} = 1$, as they are stabilized through the PNIPAAm corona (Scheme 1).

Core-crosslinked xBMANaDq precursor micelles and $ANa_{27}NIPAAm_{150}$ were mixed at pH 10 and $Z_{-/+} = 1$. The corresponding DLS CONTIN plots of the core-crosslinked precursor micelles and the resulting IPEC particles are shown in Fig. 7A. With $\langle R_h \rangle_z$ = 99 nm, the core-crosslinked IPECs are smaller than the precursor micelles due to the collapse of the PDMAEMAq corona upon IPEC formation. The hydrophilic PNIPAAm corona stabilizes the formed IPECs even at $Z_{-/+} = 1$. A schematic depiction of the proposed solution structure is shown in Fig. 7C. Fig. 7B displays a cryo-TEM micrograph of the structures at $Z_{-/+} = 1$, showing narrowly distributed IPEC particles with a uniform core size.

Next, we investigated the thermo-responsive properties of the micellar IPECs with PNIPAAm corona at $Z_{-/+} = 1$. Cloud points, T_{cl}, of the micellar solutions (c = 0.5 g L^{-1} for PANa-*b*-PNIPAAm and $c \sim 0.3$ g L^{-1} for the micellar IPEC) were determined *via* turbidity measurements applying a constant heating rate (0.15 K min^{-1}). The measurements were conducted in pH 10 buffer solutions to avoid changes of the pH with increasing temperature. The cloud points were obtained as the intersections of the tangents at the onset of turbidity. First, we performed a turbidity measurement of the $ANa_{27}NIPAAm_{150}$ diblock copolymer in pH 10 buffer solution (Fig. 8A) showing a cloud point of 38 °C.

Comparable turbidity measurements were performed for the micellar IPECs of xBMANaDq and $ANa_{27}NIPAAm_{150}$ at $Z_{-/+} = 1$ (Fig. 8B). Here, a cloud point of 34 °C was observed, comparable to the obtained value for the "free" diblock copolymer. We further carried out temperature-dependent DLS measurements to confirm the cloud point of the micellar IPECs determined *via* turbidimetry. The IPEC solution was gradually heated in steps of 2 K with an equilibration time of 5 minutes before each measurement. As shown in Fig. 9A, the hydrodynamic radius of the micellar IPECs increased distinctly when heated above ~34 °C and the IPECs precipitated. At $T > T_{cl}$, two populations can be seen in the intensity-weighted DLS CONTIN plot for T = 36 °C (inset in Fig. 9A). We tentatively assign the first population with $R_{h,app}$ = 63 nm to individual micellar IPECs with a collapsed PNIPAAm corona. The second population with $R_{h,app}$ = 517 nm might originate from the aggregation of the same structures under these conditions. The results are in good agreement with comparable measurements for micellar IPECs from non-crosslinked BMANaDq micelles and $ANa_{27}NIPAAm_{150}$ at $Z_{-/+} = 1$ (Fig. S3, ESI†). Here, a cloud point of 36 °C (Fig. S4†) was observed.

We further investigated whether this thermo-responsive behavior is fully reversible. Therefore, temperature-dependent DLS measurements were carried out for five consecutive heating and cooling cycles, in which the IPEC solution was gradually heated from 20 °C to 42 °C in steps of 2 K as described before and then directly cooled to 20 °C. Fig. 9B shows the apparent hydrodynamic radii obtained at 20 °C and 42 °C for each cycle. At 42 °C only the first population of aggregates with $R_{h,app} \sim$ 900 nm is shown for simplicity reasons, as it corresponds to the major fraction of aggregates. After cooling to 20 °C, the micellar IPECs resume their original size of $\langle R_h \rangle_z$ = 99 nm for all five cycles, indicating that the thermo-responsive behavior is reversible. In this way, we demonstrate that thermo-responsive, uniform, and multi-layered micellar IPECs can be prepared *via* the complexation of bis-hydrophilic block copolymers by core-crosslinked precursor micelles.

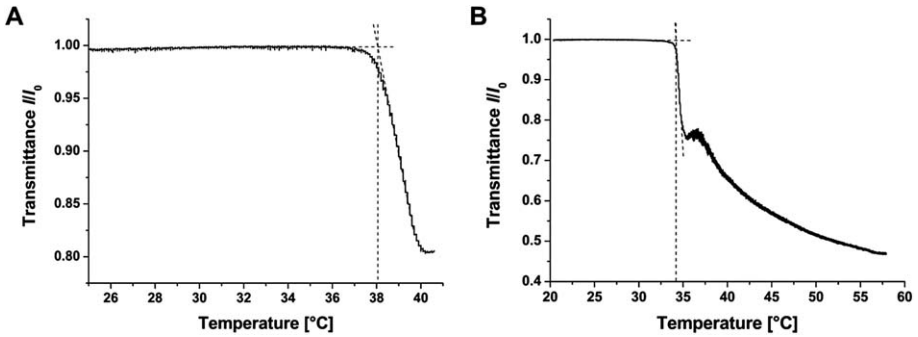

Fig. 8 Cloud point determination for $ANa_{27}NIPAAm_{150}$ ($c = 0.5$ g L^{-1}) (A) and micellar IPECs from core-crosslinked xBMANaDq precursor micelles and $ANa_{27}NIPAAm_{150}$ at $Z_{-/+} = 1$ ($c \sim 0.3$ g L^{-1}) (B) in aqueous solution at pH 10 *via* turbidity measurements.

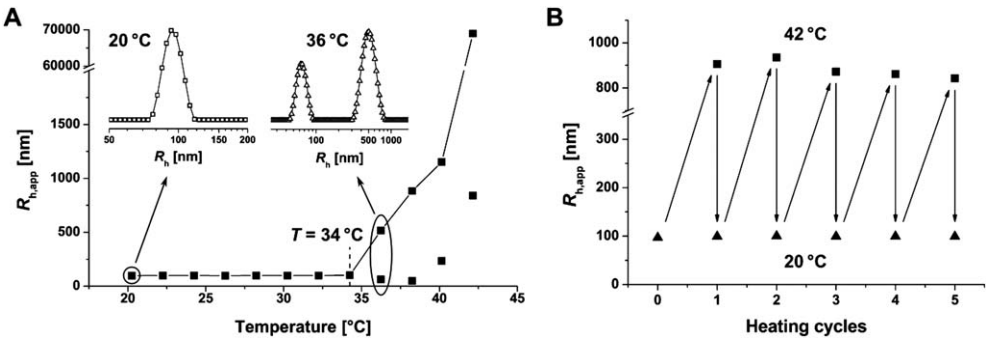

Fig. 9 Dependence of hydrodynamic radius on the temperature for micellar IPECs from core-crosslinked xBMANaDq precursor micelles and $ANa_{27}NIPAAm_{150}$ at $Z_{-/+} = 1$ ($c \sim 0.3$ g L^{-1}) in aqueous solution at pH 10 as determined by DLS (A); the insets show intensity-weighted DLS CONTIN plots for the micellar IPECs at different temperatures: 20 °C (-□-, $\langle R_h \rangle_z = 99$ nm, PDI = 0.08) and 36 °C (-△-, $R_{h,app} = 63$ nm and 517 nm); the onset of aggregation is highlighted at 34 °C; dependence of hydrodynamic radius for various temperature cycles from 20 °C (-▲-, $\langle R_h \rangle_z = 99$ nm) to 42 °C (-■-, $R_{h,app} \sim 900$ nm, only the first population of aggregates is shown) as determined by DLS (B).

Conclusion

We have successfully prepared multi-layered particles through the ionic complexation of positively charged BMANaDq triblock terpolymer micelles with negatively charged homopolymers or diblock copolymers, PSSNa and PANa-*b*-PNIPAAm. Mixing of the components in aqueous solution at high pH resulted in the formation of micellar IPECs, apparently with a ternary IPEC shell (in the case of PSSNa) or with two IPEC shells (in the case of PANa-*b*-PNIPAAm). The initial BMANaDq terpolymer micelles comprising an *im*-IPEC shell exhibited significant dynamic behavior upon complexation, resulting in changes in both the core size distribution and the aggregation number. We attribute these rearrangements to micellar fusion/fission processes, enabled by the soft core-forming block, PB. Hydrophobic bridges observed between the micellar PB cores could further trigger these dynamic processes. Under the applied conditions the dynamic nature of the micellar system was preserved upon different changes regarding the nature of the polyanion (weak or strong), its polydispersity, its composition (homopolymers or diblock copolymer), and the mixing rate of polyanion and polycation (conventional or ultrafast). Crosslinking of the PB core, on the other hand, represents a facile way to suppress such dynamics. Any complexations performed for the core-crosslinked micelles led to well-defined, uniform IPEC particles, and the core radius remained constant as shown by a detailed investigation using cryo-TEM. We further demonstrated that such micellar IPECs could be "equipped" with thermo-responsive properties, as realized *via* complexation with bis-hydrophilic diblock copolymers, PANa-*b*-PNIPAAm, and the formation of particles with a PNIPAAm corona.

In combination with our recent work on BMANaDq micelles, this micellar system shows multi-stimuli-responsive properties and dynamic behavior in response to external triggers, both in solution[28] as well as after the immobilization on surfaces.[54,55] As in both cases crosslinking of the micellar core succeeded in suppressing any rearrangements, the soft nature of the PB core enables these dynamic processes. Here, we could further demonstrate that this charged micellar system provides a straightforward building block for the generation of multi-layered nanostructures (as well as stimuli-responsive polyelectrolyte multilayers)[56] that could easily be functionalized, *e.g.*, with stimuli-responsive properties, by choosing appropriate block copolymers for complexation. In this way, the micelles could be promising candidates for smart trigger and release systems, both in solution and in thin films.

Acknowledgements

The authors thank Dr. Pierre E. Millard for the synthesis of the PAA-*b*-PNIPAAm diblock copolymer. E. B. gratefully

acknowledges funding by the state of Bavaria through a BayEFG scholarship and support by the Elite Network of Bavaria. F. H. S. is grateful for a starting independent researcher fellowship (Verband der chemischen Industrie, VCI). F. H. S. also thanks the Thuringian Ministry for Education, Science, and Culture (TMBWK; grants #B514-09051, NanoConSens, and #B515-10065, ChaPoNano) for financial support. D.V.P. acknowledges the Deutsche Forschungsgemeinschaft (DFG) for the support of his stays at the University of Bayreuth.

References

1 E. Tsuchida, Y. Osada and K. Sanada, *J. Polym. Sci., Part A: Polym. Chem.*, 1972, **10**, 3397–3404.
2 V. A. Kabanov and A. B. Zezin, *Pure Appl. Chem.*, 1984, **56**, 343–354.
3 A. F. Thünemann, M. Müller, H. Dautzenberg, J. F. O. Joanny and H. Löwen, *Adv. Polym. Sci.*, 2004, **166**, 113–171.
4 V. A. Kabanov, *Russ. Chem. Rev.*, 2005, **74**, 3–20.
5 D. V. Pergushov, O. V. Borisov, A. B. Zezin and A. H. E. Müller, *Adv. Polym. Sci.*, 2011, **241**, 131–161.
6 J. van der Gucht, E. Spruijt, M. Lemmers and M. A. Cohen Stuart, *J. Colloid Interface Sci.*, 2011, **361**, 407–422.
7 V. A. Kabanov, A. B. Zezin, V. A. Kasaikin, A. A. Yaroslavov and D. A. Topchiev, *Russ. Chem. Rev.*, 1991, **60**, 288–291.
8 G. Decher, *Science*, 1997, **277**, 1232–1237.
9 F. Caruso, R. A. Caruso and H. Möhwald, *Science*, 1998, **282**, 1111–1114.
10 A. V. Kabanov and V. A. Kabanov, *Bioconjugate Chem.*, 1995, **6**, 7–20.
11 S. Katayose and K. Kataoka, *Bioconjugate Chem.*, 1997, **8**, 702–707.
12 T. K. Bronich, H. K. Nguyen, A. Eisenberg and A. V. Kabanov, *J. Am. Chem. Soc.*, 2000, **122**, 8339–8343.
13 Y. Lee and K. Kataoka, *Soft Matter*, 2009, **5**, 3810–3817.
14 N. Lefèvre, C.-A. Fustin and J.-F. Gohy, *Macromol. Rapid Commun.*, 2009, **30**, 1871–1888.
15 I. K. Voets, A. de Keizer and M. A. Cohen Stuart, *Adv. Colloid Interface Sci.*, 2009, **147–148**, 300–318.
16 A. V. Kabanov, T. K. Bronich, V. A. Kabanov, K. Yu and A. Eisenberg, *Macromolecules*, 1996, **29**, 6797–6802.
17 M. A. Cohen Stuart, N. A. M. Besseling and R. G. Fokkink, *Langmuir*, 1998, **14**, 6846–6849.
18 J.-F. Gohy, S. K. Varshney, S. Antoun and R. Jérôme, *Macromolecules*, 2000, **33**, 9298–9305.
19 A. Harada and K. Kataoka, *Macromolecules*, 1995, **28**, 5294–5299.
20 J.-F. Gohy, S. K. Varshney and R. Jérôme, *Macromolecules*, 2001, **34**, 3361–3366.
21 I. K. Voets, A. de Keizer, P. de Waard, P. M. Frederik, P. H. H. Bomans, H. Schmalz, A. Walther, S. M. King, F. A. M. Leermakers and M. A. Cohen Stuart, *Angew. Chem., Int. Ed.*, 2006, **45**, 6673–6676.
22 D. V. Pergushov, E. V. Remizova, J. Feldthusen, A. B. Zezin, A. H. E. Müller and V. A. Kabanov, *J. Phys. Chem. B*, 2003, **107**, 8093–8096.
23 D. V. Pergushov, E. V. Remizova, M. Gradzielski, P. Lindner, J. Feldthusen, A. B. Zezin, A. H. E. Müller and V. A. Kabanov, *Polymer*, 2004, **45**, 367–378.
24 J.-F. Lutz, S. Geffroy, H. von Berlepsch, C. Böttcher, S. Garnier and A. Laschewsky, *Soft Matter*, 2007, **3**, 694–698.
25 M. G. Kellum, A. E. Smith, S. Kirkland-York and C. L. McCormick, *Macromolecules*, 2010, **43**, 7033–7040.
26 M. Burkhardt, M. Ruppel, S. Tea, M. Drechsler, R. Schweins, D. V. Pergushov, M. Gradzielski, A. B. Zezin and A. H. E. Müller, *Langmuir*, 2008, **24**, 1769–1777.
27 F. Schacher, A. Walther and A. H. E. Müller, *Langmuir*, 2009, **25**, 10962–10969.
28 E. Betthausen, M. Drechsler, M. Förtsch, F. H. Schacher and A. H. E. Müller, *Soft Matter*, 2011, **7**, 8880–8891.
29 F. H. Schacher, T. Rudolph, M. Drechsler and A. H. E. Müller, *Nanoscale*, 2011, **3**, 288–297.
30 F. Schacher, E. Betthausen, A. Walther, H. Schmalz, D. V. Pergushov and A. H. E. Müller, *ACS Nano*, 2009, **3**, 2095–2102.
31 C. V. Synatschke, F. H. Schacher, M. Förtsch, M. Drechsler and A. H. E. Müller, *Soft Matter*, 2011, **7**, 1714–1725.
32 F. Schacher, J. Yuan, H. G. Schoberth and A. H. E. Müller, *Polymer*, 2010, **51**, 2021–2032.
33 P.-E. Millard, L. Barner, J. Reinhardt, M. R. Buchmeiser, C. Barner-Kowollik and A. H. E. Müller, *Polymer*, 2010, **51**, 4319–4328.
34 T. Hofe, A. Maurer and A. H. E. Müller, *GIT Labor-Fachz.*, 1998, **42**, 1127.
35 D. Baskaran and A. H. E. Müller, *Macromolecules*, 1997, **30**, 1869–1874.
36 H. G. Schild, *Prog. Polym. Sci.*, 1992, **17**, 163–249.
37 M. M. Mok and T. P. Lodge, *J. Polym. Sci., Part B: Polym. Phys.*, 2012, **50**, 500–515.
38 A. Walther and A. H. E. Müller, *Chem. Commun.*, 2009, 1127–1129.
39 H. A. van der Schee and J. Lyklema, *J. Phys. Chem.*, 1984, **88**, 6661–6667.
40 M. R. Böhmer, O. A. Evers and J. M. H. M. Scheutjens, *Macromolecules*, 1990, **23**, 2288–2301.
41 G. B. Sukhorukov, E. Donath, S. Davis, H. Lichtenfeld, F. Caruso, V. I. Popov and H. Möhwald, *Polym. Adv. Technol.*, 1998, **9**, 759–767.
42 J. B. Schlenoff and S. T. Dubas, *Macromolecules*, 2001, **34**, 592–598.
43 M. R. Talingting, U. Voigt, P. Munk and S. E. Webber, *Macromolecules*, 2000, **33**, 9612–9619.
44 V. A. Izumrudov, A. P. Savitskii, K. N. Bakeev, A. B. Zezin and V. A. Kabanov, *Makromol. Chem., Rapid Commun.*, 1984, **5**, 709–714.
45 K. N. Bakeev, V. A. Izumrudov, S. I. Kuchanov, A. B. Zezin and V. A. Kabanov, *Macromolecules*, 1992, **25**, 4249–4254.
46 P. S. Chelushkin, E. A. Lysenko, T. K. Bronich, A. Eisenberg, V. A. Kabanov and A. V. Kabanov, *J. Phys. Chem. B*, 2008, **112**, 7732–7738.
47 Y. Li, T. K. Bronich, P. S. Chelushkin and A. V. Kabanov, *Macromolecules*, 2008, **41**, 5863–5868.
48 Z. G. Gulyaeva, M. F. Zansokhova, Y. F. Razvodovskii, V. S. Yefimov, A. B. Zezin and V. A. Kabanov, *Vysokomol. Soedin., Ser. A*, 1983, **25**, 1238–1244.
49 S. A. Sukhishvili, E. Kharlampieva and V. Izumrudov, *Macromolecules*, 2006, **39**, 8873–8881.
50 S. T. Dubas and J. B. Schlenoff, *Langmuir*, 2001, **17**, 7725–7727.
51 H. W. Jomaa and J. B. Schlenoff, *Langmuir*, 2005, **21**, 8081–8084.
52 V. A. Izumrudov, T. K. Bronich, O. S. Saburova, A. B. Zezin and V. A. Kabanov, *Makromol. Chem., Rapid Commun.*, 1988, **9**, 7–12.
53 A. Walther, A. S. Goldmann, R. S. Yelamanchili, M. Drechsler, H. Schmalz, A. Eisenberg and A. H. E. Müller, *Macromolecules*, 2008, **41**, 3254–3260.
54 J. Gensel, E. Betthausen, C. Hasenöhrl, K. Trenkenschuh, M. Hund, F. Boulmedais, P. Schaaf, A. H. E. Müller and A. Fery, *Soft Matter*, 2011, **7**, 11144–11153.
55 J. Gensel, T. Borke, N. Pazos-Pérez, A. Fery, D. V. Andreeva, E. Betthausen, A. H. E. Müller, H. Möhwald and E. V. Skorb, *Adv. Mater.*, 2012, **24**, 985–989.
56 J. Gensel, I. Dewald, J. Erath, E. Betthausen, A. H. E. Müller and A. Fery, *Chem. Sci.*, submitted.